Effect of Na adsorption on the structural and electronic properties of Si(111)$\sqrt{3} \times \sqrt{3}$ -Au surface

2014 J. Phys.: Condens. Matter 26 055009

(http://iopscience.iop.org/0953-8984/26/5/055009)

IOP Publishing Journal of Physics: Condensed Matter
J. Phys.: Condens. Matter **26** (2014) 055009 (7pp) doi:10.1088/0953-8984/26/5/055009

Effect of Na adsorption on the structural and electronic properties of Si(111)$\sqrt{3} \times \sqrt{3}$-Au surface

L V Bondarenko[1,2], A V Matetskiy[1,2], A A Yakovlev[1,2], A Y Tupchaya[1,2], D V Gruznev[1,2], M V Ryzhkova[1,2], D A Tsukanov[1,2], E A Borisenko[1], E N Chukurov[1], N V Denisov[1,2], O Vilkov[3], D V Vyalikh[3,4], A V Zotov[1,2,5] and A A Saranin[1,2]

[1] Institute of Automation and Control Processes FEB RAS, 690041 Vladivostok, Russia
[2] School of Natural Sciences, Far Eastern Federal University, 690950 Vladivostok, Russia
[3] St Petersburg State University, 198504 St Petersburg, Russia
[4] Institute of Solid State Physics, Dresden University of Technology, D-01062 Dresden, Germany
[5] Department of Electronics, Vladivostok State University of Economics and Service, 690600 Vladivostok, Russia

E-mail: saranin@iacp.dvo.ru

Received 2 October 2013, revised 2 December 2013
Accepted for publication 6 December 2013
Published 16 January 2014

Abstract

Adsorption of ~0.1 ML of Na onto the Si(111)$\sqrt{3} \times \sqrt{3}$-Au surface held at 300 °C has been found to induce pronounced changes in its structural and electronic properties. Domain wall networks, characteristic of the pristine surface, are removed completely, leading to the formation of a highly ordered homogeneous surface. The original atomic arrangement of the Si(111)$\sqrt{3} \times \sqrt{3}$-Au is preserved and Na atoms occupy T_4 adsorption sites at the centers of surface Si trimers. Upon Na adsorption, a pronounced metallic S_1 surface-state band develops. It is characterized by a large spin splitting (momentum splitting at the Fermi level $\Delta k_{\parallel} = 0.027$ Å^{-1} and consequent energy splitting $\Delta E_F = 110$ meV), large electron filling (on the order of 0.5 electrons per $\sqrt{3} \times \sqrt{3}$ unit cell) and small effective electron mass of $(0.028 \pm 0.006)m_e$. The natural consequence of the latter properties is a high surface conductivity of the Si(111)$\sqrt{3} \times \sqrt{3}$-(Au, Na) surface.

Keywords: atom–solid interactions, electronic band structure, scanning tunneling microscopy, angle-resolved photoemission, surface reconstructions

(Some figures may appear in colour only in the online journal)

1. Introduction

Silicon surfaces covered with monoatomic and sub-monoatomic layers of metals (i.e., metal/silicon reconstructions) have attracted considerable attention due to the variety of structural and electronic properties. In particular, such overlayers can show up as two-dimensional electron–gas systems, i.e. exhibit the properties of the extrathin two-dimensional metals. When dealing with heavy metals, where spin–orbit interaction is noticeable, one could expect splitting of the surface-state bands due to the surface Rashba effect [1, 2]. Indeed, a large Rashba splitting has already been found on a set of metal/silicon reconstructions, Bi/Si(111) [3–5], Tl/Si(111) [6, 7], and Pt/Si(110) [8], but it appeared to occur only in the insulating surface-state bands. In contrast, spin-split metallic bands are demanded, bearing in mind any spintronic device applications. The first metal/semiconductor system with a spin splitting of a metallic surface-state band to be found was Pb/Ge(111) [9, 10] followed by Au/Ge(111) [11–13]. Recently, we have demonstrated that large spin splitting

of metallic surface-state bands can be obtained on silicon with adsorbate-modified Au/Si(111) reconstructions [14]. It has been found that a structurally and electronically poor Au/Si(111)$\sqrt{3} \times \sqrt{3}$ surface (due to a presence of random domain walls) is substantially improved by adsorbing small amounts of suitable species (e.g., Tl, In, Cs, Na). As a result, highly ordered homogeneous surfaces are formed with pronounced spin-split metallic surface-state bands.

In the present study, we have characterized the structural and electronic properties of the Na-modified Au/Si(111)$\sqrt{3} \times \sqrt{3}$ surface in detail using a range of experimental techniques (scanning tunneling microscopy (STM), low-energy electron diffraction (LEED), x-ray photoelectron spectroscopy (XPS), angle-resolved photoelectron spectroscopy (ARPES), four-point-probe (4pp) conductivity measurements) and DFT calculations. Questions under consideration include the sodium adsorption site, the relaxed atomic structure of the surface, Na-induced changes of the surface-state bands and surface-atom core levels, and the effect of Na on the surface conductivity.

2. Experimental and calculation details

Experiments were performed with an Omicron MULTIPROBE ARPES system operated in an ultrahigh vacuum ($\sim 2.5 \times 10^{-10}$ mbar). Atomically clean Si(111)7 × 7 surfaces were prepared *in situ* by flashing to 1280 °C after the samples were first outgassed at 600 °C for several hours. Gold was deposited from a heated Au-covered W wire at a rate of about 0.5 ML min^{-1}. Sodium was deposited from a well-outgassed commercial SAES chromate dispenser. The Na coverage was estimated from STM and LEED observations of the well-established Si(111)3 × 1-Na reconstruction with a saturation coverage of 1/3 ML [15]. For estimation of the Au deposition rate, the Si(111)5 × 2-Au reconstruction, which has a coverage of 0.6 ML [16], was taken as a reference. For STM observations, electrochemically etched tungsten tips cleaned by *in situ* heating were employed. The STM images were acquired in a constant-current mode after cooling the sample to room temperature or 110 K. ARPES measurements were conducted using a hemispherical electron analyzer VG Scienta R3000. The light source was a high-flux monochromatized He discharge lamp with a photon energy of 21.2 eV. Also, ARPES and XPS measurements were performed at UE56/2-PGM-2 and the Russian–German beamline of the BESSY-II synchrotron radiation facility, respectively. For ARPES measurements samples were cryogenically cooled down to 78 K.

To elucidate Na adsorption geometry on the Au/Si(111) $\sqrt{3} \times \sqrt{3}$ surface, plane-wave total energy calculations were performed using the Vienna *ab initio* simulation package (VASP) [17–20] based on density functional theory (DFT) [21] with projector-augmented wave (PAW) pseudopotentials [22]. The local density approximation (LDA) after Ceperley–Alder [23] in the Perdew–Zunger parametrization [24] for the exchange and correlation functional have been employed. The electronic wavefunctions were expanded in a plane-wave basis set with an energy cutoff of 20 Ryd. The surface was simulated by a periodic slab geometry with a $2\sqrt{3} \times 2\sqrt{3}$-Au supercell containing nine Si atomic layers (each one containing 12 Si atoms) and a top Au layer (12 Au atoms). The dangling bonds of the bottom slab layer were saturated by hydrogen atoms. The hydrogen atoms and bottom bilayer silicon atoms were fixed and the remaining atoms were free to move. A vacuum region of approximately 15 Å was incorporated within each periodic unit cell to prevent interactions between adjacent surfaces. The geometry was optimized until the total energy converged to 10^{-4} eV and the total force converged to 10^{-3} eV Å^{-1}. The sensitivity of the formation energies on the kinetic energy cutoff, *k*-points setup, and the total energy/force numerical accuracy has been tested and found to have a negligible effect on the total energy differences.

3. Results and discussion

Figure 1 illustrates the main effect of saturating Na adsorption at ∼300 °C on the structure of the Si(111)-$\sqrt{3} \times \sqrt{3}$-Au surface. The pristine Si(111)$\sqrt{3} \times \sqrt{3}$-Au surface exists in two forms, denoted as the α-$\sqrt{3} \times \sqrt{3}$ phase and the β-$\sqrt{3} \times \sqrt{3}$ phase [25]. Both phases have qualitatively similar structural arrangements, consisting of commensurate $\sqrt{3} \times \sqrt{3}$ domains separated by meandering domain walls (DWs). The difference between the α-phase and β-phase is determined simply by the density of the DWs. While in the case of α-$\sqrt{3} \times \sqrt{3}$-Au the domains are relatively large (sub-100 Å) and, thus, are clearly seen in STM images, the β-$\sqrt{3} \times \sqrt{3}$ phase is essentially a dense disordered array of DWs having a rather complicated STM appearance. The $\alpha \rightarrow \beta$ transition takes place gradually in the course of Au deposition [26, 25] since the local coverage in a DW is higher than that in a commensurate domain [27]. In the present study we have found that both phases demonstrate similar behavior upon Na adsorption and the resulting surfaces are virtually the same, despite a certain difference in the initial Au coverage. A typical Au/Si(111) surface used in the present study is shown in figure 1(a). It is basically the β-phase with a few inclusions of the α-phase. The LEED pattern from such a surface corresponds to the well-defined β-$\sqrt{3} \times \sqrt{3}$ one, in agreement with the earlier LEED observations [28, 29]. For simplicity, we denote the pristine surface just as $\sqrt{3} \times \sqrt{3}$-Au.

After Na adsorption at 300 °C, domain walls are completely eliminated and a highly ordered homogeneous surface is seen in the STM images (figure 1(b)). Consequently, a sharp $\sqrt{3} \times \sqrt{3}$ LEED pattern without any other features develops. These observations are very similar to those obtained with adsorption of the other species, such as In, Tl, and Cs onto the Si(111)-$\sqrt{3} \times \sqrt{3}$-Au surface [30, 28], and the homogeneous Si(111)$\sqrt{3} \times \sqrt{3}$-(Au, Na) surface can be also denoted as the *h*-$\sqrt{3} \times \sqrt{3}$ phase (*h* means homogeneous) by analogy with the *h*-$\sqrt{3} \times \sqrt{3}$-(Au, In) [28].

The similarity between various *h*-$\sqrt{3} \times \sqrt{3}$ surfaces is preserved also for low-temperature (LT) observations, where random arrays of 'frozen' adatoms are seen in all cases. Figure 1(c) presents the LT-STM image of a surface similar to that shown in the room-temperature STM image in figure 1(b) after it has been cooled to 110 K. However, unlike the group-III elements (In and Tl), Na adatoms do not form any regular lattice at LT. The Fourier pattern from this surface

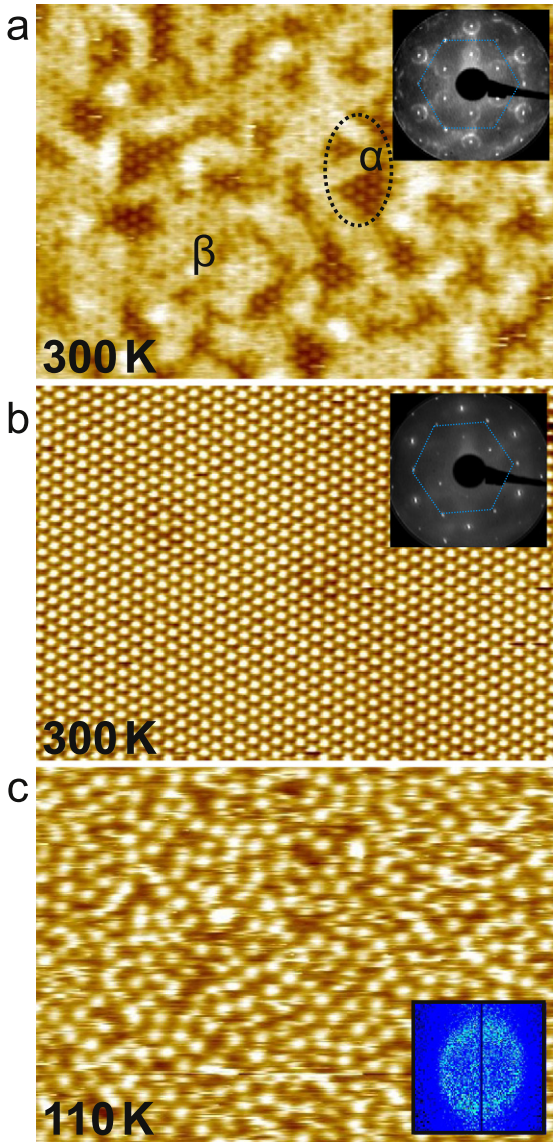

Figure 1. Homogenizing effect of sodium adsorption on the Au/Si(111) surface structure. (a) Room-temperature (RT) STM image (+1.8 V, 0.1 nA) and LEED pattern of the pristine Si(111)-$\sqrt{3} \times \sqrt{3}$-Au surface. The surface comprises an β-phase with inclusions of α-phase (indicated as a dotted ellipse). (b) RT-STM image (−1.2 V, 1.0 nA) and LEED pattern of the same surface after saturating adsorption of ∼0.1 ML of Na onto it at 300 °C. (c) Low-temperature (110 K) STM image (−2.0 V, 0.3 nA) and the FFT pattern of the same surface as in (b). STM image scale: 250×180 Å^2. Blue hexagons in LEED patterns mark positions of bulk (1×1) spots.

(inset in figure 1(c)) displays a smeared ring, indicating an azimuthal disordering. The average spacing between Na adatoms is $2\sqrt{3}a$, as determined from STM line profiles and confirmed by the radius of the ring in the Fourier pattern. Such an average spacing yields an estimate for Na coverage of $\sim 1/12 \simeq 0.08$ ML. This value agrees with the result of a direct counting of Na-associated protrusions in the LT-STM images, which yields about 0.1 ML of Na.

Comparing the RT-STM appearance of the h-$\sqrt{3}$-(Au, Na) surface with that of the Group-III-adsorbed surfaces, h-$\sqrt{3}$-(Au, In) [30] and h-$\sqrt{3}$-(Au, Tl) [14], one can notice an

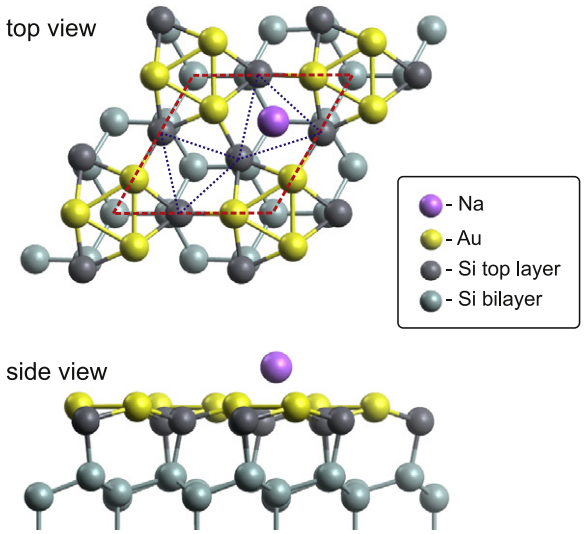

Figure 2. Atomic model of the Si(111)-$\sqrt{3} \times \sqrt{3}$-Au reconstruction with one incorporated Na atom per $2\sqrt{3} \times 2\sqrt{3}$ unit cell. The $\sqrt{3} \times \sqrt{3}$ unit cell is outlined with a red rhombus, Si trimers are indicated by blue triangles.

essential difference. While the latter display a honeycomb-like structure [30, 14] (with two protrusions per $\sqrt{3} \times \sqrt{3}$ unit cell), the former shows up as a hexagonal array with a single protrusion per $\sqrt{3} \times \sqrt{3}$ unit cell (figure 1(b)). Note that unit cell of the $\sqrt{3} \times \sqrt{3}$-Au structure described by the conjugated honeycomb chained trimer (CHCT) model [31] contains two equivalent conjugated Si trimers centered in the T_4 sites and a single Au trimer centered in the other T_4 site. For the h-$\sqrt{3}$-(Au, In) surface, In-atom occupation of the T_4 site in the Si-trimer center was found to be the most stable adsorption configuration [30, 28, 32]. The honeycomb appearance of the h-$\sqrt{3}$-(Au, In) surface was concluded to reflect the averaged pattern produced by mobile In atoms (∼0.15 ML) visiting all the above adsorption sites [30]. Taking into account the different chemical nature of alkali metal Na as compared to Group-III In, as well as the difference in the RT-STM appearance of the corresponding h-$\sqrt{3}$ surfaces, one could expect that Na might occupy the other adsorption site.

To check this possibility, we have examined the energetics of Na adsorption in various adsorption sites at the $\sqrt{3} \times \sqrt{3}$-Au surface using DFT calculations. The main result of this consideration is that the most energetically favorable adsorption site for Na is that over the Si trimer. In particular, this configuration is by ∼0.3 eV more stable than that with a Na atom on top of the Au trimer.

Figure 2 shows the relaxed model of the h-$\sqrt{3} \times \sqrt{3}$-(Au, Na) surface. The presence of the Na atom induces a minor distortion in the Au trimer, whose sides (2.86 Å) change by less than 0.02 Å. On the other hand, the Si trimers demonstrate a slightly greater responsiveness. Originally, both Si trimers are equal, with a Si–Si bond length of 3.51 Å. After one Si trimer is occupied by the Na atom the Si–Si bond length in it increases to 3.65 Å accompanied by squeezing and distortion of the other Si trimer, whose sides change to 3.43, 3.46 and 3.50 Å.

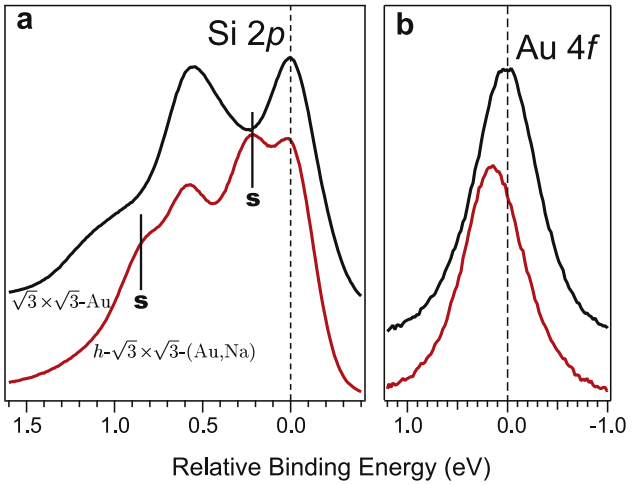

Figure 3. XPS spectra obtained with a photon energy of 135 eV for (a) Si 2p and (b) Au 4f core levels of the pristine $\sqrt{3} \times \sqrt{3}$-Au surface (black line) and h-$\sqrt{3} \times \sqrt{3}$-(Au, Na) surface (red line). Developing surface-related components in the Si 2p spectrum from the h-$\sqrt{3} \times \sqrt{3}$-(Au, Na) surface are indicated by the character 's'.

Results of the XPS study on the effect of Na on the core-level structure of the $\sqrt{3} \times \sqrt{3}$-Au surface are summarized in figure 3. Upon Na adsorption, the Au 4f peak undergoes a marginal shift of ∼120 meV towards a higher binding energy (figure 3(b)). In the Si 2p spectrum, additional higher-energy components (labeled 's' in figure 3(a)) appear with Na adsorption. When the emission angle was lowered by 23° from the normal direction the intensity of these components increased relative to the major 2p peaks, indicating that they are surface related. These changes in the Au 4f and Si 2p spectra are very similar to those reported for the In/$\sqrt{3} \times \sqrt{3}$-Au surface in [28], where they were interpreted as a sign of the direct interaction of In adsorbates with the surface Si atoms in contrast to Au atoms. However, with electron transfer from Na adsorbates towards Si atoms, one would expect the chemical shift of the Si 2p peak in the opposite direction (i.e., to the lower binding energies). The essential band bending effect can also be ruled out, as it would result in a rigid shift of all peaks. Hence, the most plausible origin of the observed shifts of the Au 4f and surface Si 2p peaks is related to core-hole screening [33, 34] enhanced by filling of the S_1 band and the development of a perfect two-dimensional electron–gas system.

Figure 4 illustrates the effect of Na adsorption on the surface band dispersion of Si(111)$\sqrt{3} \times \sqrt{3}$-Au, as revealed with ARPES. One can see that upon Na adsorption all available spectral features (e.g., S_2, S_3 surface bands [29, 35, 28] and light-hole (LH) band of the inversion layer [36]) become noticeably sharp and go down to a higher binding energy and an almost linear dispersion feature appears around the center of the surface Brillouin zone ($\bar{\Gamma}$), corresponding to the S_1 surface state which is usually invisible at $k^{\parallel} = 0$ for the pristine $\sqrt{3} \times \sqrt{3}$-Au surface [35]. The most principal Na-induced spectral changes are associated with electron filling and shifting down of the metallic S_1 band, while the other bands are also shifted, but to a lesser extent, similarly to the effects produced by In adsorbate [28].

The same band recorded around the second $\bar{\Gamma}$ point (i.e., $\bar{\Gamma}_1$) of the $\sqrt{3} \times \sqrt{3}$ lattice in order to avoid contributions from bulk and inversion layer features is shown in figure 5. Spin splitting of the band is clearly seen (with momentum splitting at the Fermi level $\Delta k_{\parallel} = 0.027$ Å^{-1} and consequent energy splitting $\Delta E_F = 110$ meV), the origin of which and

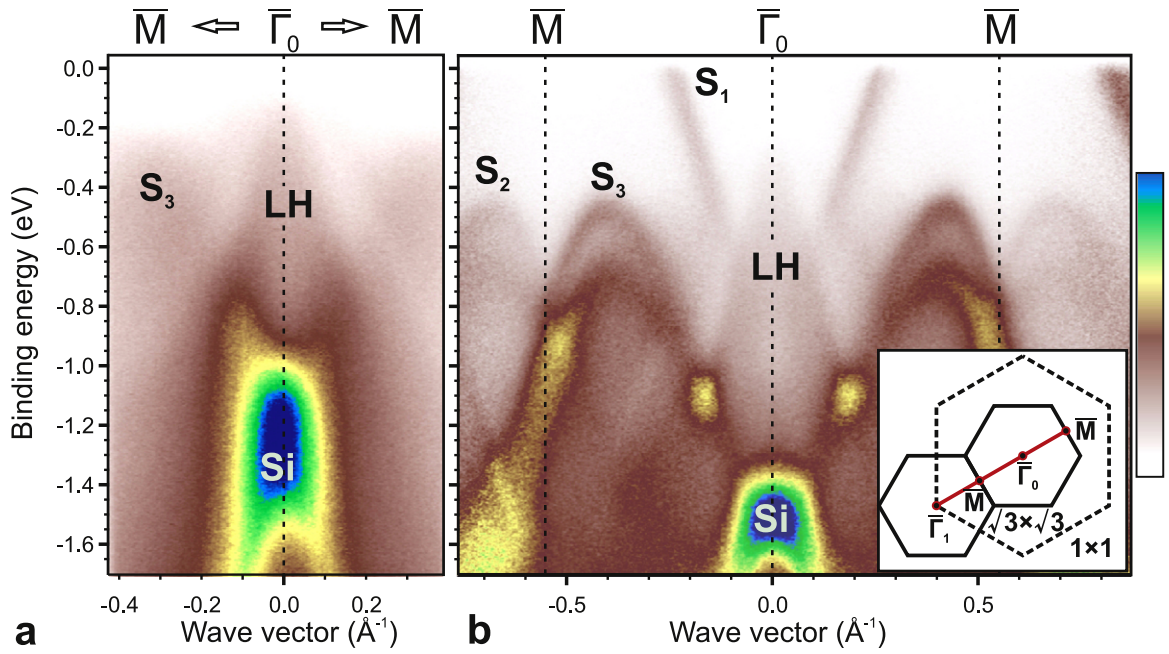

Figure 4. Surface band dispersion of the Au/Si(111) surface (a) before and (b) after ∼0.1 ML Na adsorption at ∼300 °C. ARPES spectra are taken at 78 K along the $\bar{M}$–$\bar{\Gamma}_0$–$\bar{M}$ line. Inset shows the schematic representation of bulk (1 × 1) and surface $\sqrt{3} \times \sqrt{3}$ Brillouin zones. The intensity scale is shown on the right side.

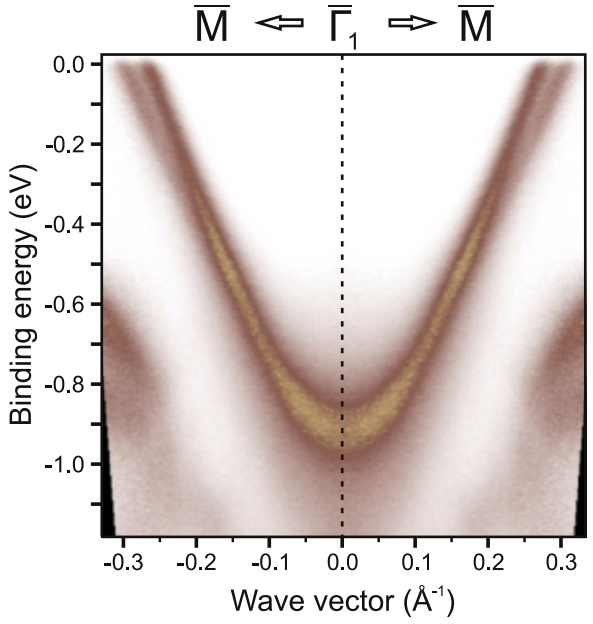

Figure 5. Symmetrized ARPES spectrum recorded along the $\bar{M}$–$\bar{\Gamma}_1$–$\bar{M}$ direction on the Na-adsorbed Au/Si(111) surface, showing dispersion of the spin-split S_1 surface-state band.

details of the spin texture are discussed elsewhere [14]. From the measured Fermi wavevector (0.28 Å^{-1}) the number of electrons in the bands can be roughly estimated as 1.25×10^{18} m^{-2}, which corresponds to 0.48 electrons per $\sqrt{3} \times \sqrt{3}$ unit cell. Taking into account the Na saturation coverage of 0.1 ML, each Na atom is estimated to donate ~1.5 electrons. (We believe that a more realistic value is about 1.0 electron per Na atom and overestimation stems from the inaccuracy of evaluating the electron band filling and from neglecting extra electron doping from excess surface Au atoms, as reported for the Au/Ge(111)$\sqrt{3} \times \sqrt{3}$ surface [37]). The slope of the band corresponds to the average Fermi velocity of about 7×10^5 m s^{-1}, which is close to the value reported for the ordered Sn–Ag alloy on Si(111) [38]. The average effective mass around the Fermi level is then determined to be (0.028 ± 0.006)m_e, where m_e is the electron rest mass. Note that this effective mass is about ten times smaller than that of the surface prior to Na adsorption (0.3m_e [28]), which seems to indicate that the S_1 band dispersion is not parabolic.

All the effects of Na adsorption, including the removal of domain walls, increasing electron filling of the metallic surface-state band and decreasing electron effective mass are expected to lead to a significant increase in the surface conductivity. This has indeed been proved with 4pp-conductivity measurements, the main results of which are summarized in table 1. One can see that the conductivities of the pristine α-$\sqrt{3}$-Au and β-$\sqrt{3}$-Au phases are similar, being around 1.4 mS. It is slightly greater for the β-$\sqrt{3}$-Au phase, possibly due to a larger Au coverage. Na-induced transformation of these phases to the h-$\sqrt{3}$-(Au, Na) surface increases the surface conductivity almost four times, up to ~5.3 mS. One could expect a greater effect, but current flowing through the sample bulk might smear the actual increase of surface-state conductivity.

Table 1. Changes in the surface conductivity during Na adsorption onto various Au/Si(111) reconstructions.

Pristine Au/Si(111)		Na-modified Au/Si(111)	
Reconstruction	S, mS	Reconstruction	S, mS
α-$\sqrt{3} \times \sqrt{3}$-Au	1.3 ± 0.1	h-$\sqrt{3} \times \sqrt{3}$-(Au, Na)	5.2 ± 0.4
β-$\sqrt{3} \times \sqrt{3}$-Au	1.5 ± 0.1	h-$\sqrt{3} \times \sqrt{3}$-(Au, Na)	5.3 ± 0.4

In the present experiments, the Na-modified h-$\sqrt{3} \times \sqrt{3}$ surface contains a saturation Na coverage of about 0.1 ML. Such a coverage seems to be far from the optimum for the $\sqrt{3} \times \sqrt{3}$ periodicity (0.33 ML, which corresponds to one atom per unit cell) and the surface gives the impression of being able to accept more Na atoms. However, any attempt to force the surface conductivity up to the higher values by introducing additional Na atoms and increasing the population of the 2D adatom gas fails. Figure 6 demonstrates the changes in the surface conductivity during RT adsorption of additional Na onto the h-$\sqrt{3} \times \sqrt{3}$-(Au, Na). The initially high conductivity rapidly falls off with increasing extra Na coverage. The disordering of the surface by redundant Na atoms is seen by both LEED (fading diffraction spots and gaining background) and ARPES. The inset in figure 6 shows the gradual fading of the metallic S_1 band accompanied by the disappearance of the S_3 band. Thus, a Na coverage of about 0.1 ML appears to be optimum for developing a h-$\sqrt{3} \times \sqrt{3}$ surface with advanced structural and electronic properties.

4. Conclusions

In conclusion, although the alkali metal Na is apparently very different from the Group-III element In, they affect the structural and electronic properties of the Au/Si(111)$\sqrt{3} \times \sqrt{3}$ surface in a similar way. In both cases, domain walls, characteristic of the pristine Si(111)$\sqrt{3}$-Au surface, are completely removed and a highly ordered homogeneous surface is formed. The surface preserves its basic atomic $\sqrt{3} \times \sqrt{3}$-Au structure, while Na atoms (like In atoms) remain as adatoms occupying T_4 adsorption sites within conjugated Si trimers. The main effect of Na and In adsorption on the electronic properties of Au/Si(111)$\sqrt{3} \times \sqrt{3}$ resides in developing a pronounced spin-split metallic surface-state band. In the case of the Na adsorbate, electron filling of this band is especially great (on the order of 0.5 electrons per $\sqrt{3} \times \sqrt{3}$ unit cell) and the effective electron mass is very small, (0.028 ± 0.006)m_e. Thus, the surface exhibits a high conductivity. This property together with a noticeable spin splitting (momentum splitting at the Fermi level $\Delta k_{\parallel} = 0.027$ Å^{-1} and consequent energy splitting $\Delta E_F = 110$ meV) makes the Na-modified Au/Si(111)$\sqrt{3} \times \sqrt{3}$ surface a promising candidate for studying spin transport in low-dimensional systems and opens prospects for using it as possible element for spintronic applications.

Acknowledgments

Experimental support from D Usachov and A Fedorov is gratefully acknowledged. Part of this work was supported by

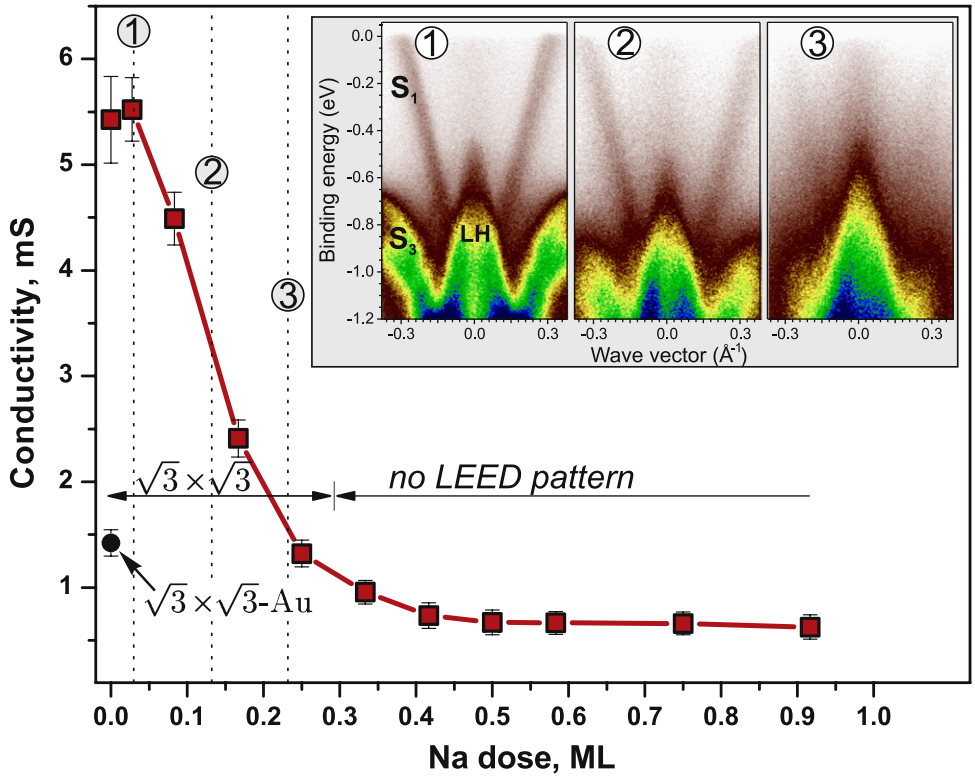

Figure 6. Evolution of the surface conductivity in the course of additional Na adsorption onto the h-$\sqrt{3}\times\sqrt{3}$-(Au, Na) surface held at RT. Conductivity of the pristine $\sqrt{3}$-Au phase is indicated by a black dot. Regions of changing LEED pattern from the $\sqrt{3}\times\sqrt{3}$ to the disordered structure are indicated. Inset shows surface band dispersion of the Na-modified Au/Si(111) surface after RT adsorption of an additional 0.03, 0.13 and 0.23 ML of Na. ARPES spectra are taken at 78 K around the $\bar{\Gamma}_0$ point.

the Russian Foundation for Basic Research (Grant Nos 13-02-00730, 13-02-00837, 13-02-12110, 12-02-31502, 12-02-31832, 12-02-00416, 12-02-31502, and 12-02-00430), and the Ministry of Education and Science of the RF (Grant Nos 8022, 8581 and 2.1004.2011) and NSh-774.2012.2. LVB thanks G-RISC for support. We acknowledge Helmholtz Zentrum Berlin für Materialien und Energie for support within a bilateral Russian–German Laboratory program.

References

[1] Rashba E I 1960 Properties of semiconductors with an extremum loop. 1. Cyclotron and combinational resonance in a magnetic field perpendicular to the plane of the loop *Sov. Phys.—Solid. State* **2** 1109

[2] Bychkov Yu A and Rashba E I 1984 Properties of a 2D electron gas with lifted spectral degeneracy *JETP Lett.* **39** 78

[3] Gierz I, Suzuki T, Frantzeskakis E, Pons S, Ostanin S, Ernst A, Henk J, Grioni M, Kern K and Ast C R 2009 Silicon surface with giant spin splitting *Phys. Rev. Lett.* **103** 046803

[4] Sakamoto K *et al* 2009 Peculiar Rashba splitting originating from the two-dimensional symmetry of the surface *Phys. Rev. Lett.* **103** 156801

[5] Frantzeskakis E, Pons S and Grioni M 2010 Band structure scenario for the giant spin–orbit splitting observed at the Bi/Si(111) interface *Phys. Rev.* B **82** 085440

[6] Sakamoto K *et al* 2009 Abrupt rotation of the Rashba spin to the direction perpendicular to the surface *Phys. Rev. Lett.* **102** 096805

[7] Ibañez-Azpiroz J, Eiguren A and Bergara A 2011 Relativistic effects and fully spin-polarized Fermi surface at the Tl/Si(111) surface *Phys. Rev.* B **84** 125435

[8] Park J, Jung S W, Jung M C, Yamane H, Kosugi N and Yeom H W 2013 Self-assembled nanowires with giant Rashba split band *Phys. Rev. Lett.* **110** 036801

[9] Yaji K, Ohtsubo Y, Hatta S, Okuyama H, Miyamoto K, Okuda T, Kimura A, Namatame H, Taniguchi M and Aruga T 2010 Large Rashba spin splitting of a metallic surface-state band on a semiconductor surface *Nature Commun.* **1** 17

[10] Yaji K, Hatta S, Aruga T and Okuyama H 2012 Structural and electronic properties of the Pb/Ge(111)-$\beta(\sqrt{3}\times\sqrt{3})$R30° surface studied by PES and first-principles calculations *Phys. Rev.* B **86** 235317

[11] Höpfner P, Schäfer J, Fleszar A, Blumenstein C, Schramm T, Heßmann M, Cui X, Patthey L, Hanke W and Claessen R 2011 Electronic band structure of the two-dimensional metallic electron system Au/Ge(111) *Phys. Rev.* B **83** 235435

[12] Nakatsuji K, Niikura R, Shibata Y, Yamada M, Iimori T, Komori F, Oda Y and Ishii A 2011 Anisotropic splitting and spin polarization of metallic bands due to spin–orbit interaction at the Ge(111)($\sqrt{3}\times\sqrt{3}$)R30°-Au surface *Phys. Rev.* B **84** 035436

[13] Höpfner P *et al* 2012 Three-dimensional spin rotations at the Fermi surface of a strongly spin–orbit coupled surface system *Phys. Rev. Lett.* **108** 186801

[14] Bondarenko L V *et al* 2013 Large spin splitting of metallic surface-state bands at adsorbate-modified gold/silicon surfaces *Sci. Rep.* **3** 1826

[15] Erwin S C 1995 New structural model for the alkali-induced Si(111)-(3 × 1) reconstruction from first principles *Phys. Rev. Lett.* **75** 1973
[16] Erwin S C, Barke I and Himpsel F J 2009 Structure and energetics of Si(111)-(5×2)-Au *Phys. Rev.* B **80** 155409
[17] Kresse G and Hafner J 1993 *Ab initio* molecular dynamics for liquid metals *Phys. Rev.* B **47** 558
[18] Kresse G and Hafner J 1994 *Ab initio* molecular-dynamics simulation of the liquid-metal–amorphous-semiconductor transition in germanium *Phys. Rev.* B **49** 14251
[19] Kresse G and Furthmüller J 1996 Efficient iterative schemes for *ab initio* total-energy calculations using a plane-wave basis set *Phys. Rev.* B **54** 11169
[20] Kresse G and Furthmüller J 1996 Efficiency of *ab-initio* total energy calculations for metals and semiconductors using a plane-wave basis set *Comput. Mater. Sci.* **6** 15
[21] Kohn W and Sham L J 1965 Self-consistent equations including exchange and correlation effects *Phys. Rev.* **140** A1133
[22] Kresse G and Joubert D 1999 From ultrasoft pseudopotentials to the projector augmented-wave method *Phys. Rev.* B **59** 1758
[23] Ceperley D M and Alder B J 1980 Ground state of the electron gas by a stochastic method *Phys. Rev. Lett.* **45** 566
[24] Perdew J P and Zunger A 1981 Self-interaction correction to density-functional approximations for many-electron systems *Phys. Rev.* B **23** 5048
[25] Nagao T, Hasegawa S, Tsuchie K, Ino S, Voges C, Klos G, Pfnür H and Henzler M 1998 Structural phase transitions of Si(111)-($\sqrt{3}\times\sqrt{3}$)R30°-Au: phase transitions in domain-wall configurations *Phys. Rev.* B **57** 10100
[26] Nogami J, Baski A A and Quate C F 1990 $\sqrt{3}\times\sqrt{3} \longrightarrow 6\times 6$ phase transition on the Au/Si(111) surface *Phys. Rev. Lett.* **65** 1611
[27] Falta J, Hille A, Novikov D, Materlik G, Seehofer L, Falkenberg G and Johnson R L 1995 Domain wall structure of Si(111)($\sqrt{3}\times\sqrt{3}$)R30°-Au *Surf. Sci.* **330** L673
[28] Kim J K, Kim K S, McChesney J L, Rotenberg E, Hwang H N, Hwang C C and Yeom H W 2009 Two-dimensional electron gas formed on the indium-adsorbed Si(111)$\sqrt{3}\times\sqrt{3}$-Au surface *Phys. Rev.* B **80** 075312
[29] Zhang H M, Balasubramanian T and Uhrberg R I G 2002 Surface electronic structure study of Au/Si(111) reconstruction: observation of crystal-to-glass transition *Phys. Rev.* B **66** 165402
[30] Gruznev D V, Filippov I N, Olyanich D A, Chubenko D N, Kuyanov I A, Saranin A A, Zotov A V and Lifshits V G 2006 Si(111)-α-$\sqrt{3}\times\sqrt{3}$-Au phase modified by In adsorption: stabilization of a homogeneous surface by stress relief *Phys. Rev.* B **73** 115335
[31] Ding Y G, Chan C T and Ho K M 1992 Theoretical investigation of the structure of the ($\sqrt{3}\times\sqrt{3}$)R30°-Au/Si(111) surface *Surf. Sci.* **275** L691
[32] Hsu C H, Lin W H, Ozolins V and Chuang F C 2012 Electronic structure of the indium-adsorbed Au/Si(111)-$\sqrt{3}\times\sqrt{3}$ surface: a first-principles study *Phys. Rev.* B **85** 155401
[33] Pehlke E and Scheffler M 1993 Evidence for site-sensitive screening of core holes at the Si and Ge(001) surface *Phys. Rev. Lett.* **71** 2338
[34] Eriksson P E J and Uhrberg R I G 2010 Surface core-level shifts on clean Si(001) and Ge(001) studied with photoelectron spectroscopy and density functional theory calculations *Phys. Rev.* B **81** 125443
[35] Altmann K N, Crain J N, Kirakosian A, Lin J L, Petrovykh D Y, Himpsel F J and Losio R 2001 Electronic structure of atomic chains on vicinal Si(111)–Au *Phys. Rev.* B **64** 035406
[36] Kim K S, Jung S C, Kang M H and Yeom H W 2010 Nearly massless electrons in the silicon interface with a metal film *Phys. Rev. Lett.* **104** 246803
[37] Nakatsuji K, Motomura Y, Niikura R and Komori F 2013 Selective doping in a surface band and atomic structures of the Ge(111)($\sqrt{3}\times\sqrt{3}$)R30°-Au surface *J. Phys.: Condens. Matter* **25** 045007
[38] Osiecki J R, Sohail H M, Eriksson P E J and Uhrberg R I G 2012 Experimental and theoretical evidence of a highly ordered two-dimensional Sn/Ag alloy on Si(111) *Phys. Rev. Lett.* **109** 057601